

**A SCHEDULING AND ROUTING ALGORITHM FOR  
DIGITAL MICROFLUIDIC RING LAYOUTS WITH  
BUS-PHASE ADDRESSING**

By

Megha Gupta

A Thesis Submitted to the Graduate  
Faculty of Rensselaer Polytechnic Institute  
in Partial Fulfillment of the  
Requirements for the Degree of  
MASTER OF SCIENCE  
Major Subject: COMPUTER SCIENCE

Approved:

---

Srinivas Akella  
Thesis Adviser

Rensselaer Polytechnic Institute  
Troy, New York

April 2008  
(For Graduation May 2008)

# CONTENTS

LIST OF FIGURES . . . . .	iii
ACKNOWLEDGMENT . . . . .	v
ABSTRACT . . . . .	vi
1. INTRODUCTION . . . . .	1
1.1 Digital Microfluidic Systems . . . . .	1
1.2 Related Work . . . . .	2
2. RING LAYOUTS WITH BUS-PHASE ADDRESSING . . . . .	5
2.1 Dual Ring Layout . . . . .	6
2.2 Synchronous Ring Layout . . . . .	6
3. THE ALGORITHM . . . . .	9
3.1 Problem Statement . . . . .	9
3.2 Applicability of the Algorithm to Different Layouts . . . . .	9
3.3 Applicability of the Algorithm to Different Reactions . . . . .	10
3.4 Overview . . . . .	12
3.5 Assumptions . . . . .	13
3.6 Injection from Sources . . . . .	13
3.7 Mixing . . . . .	14
3.8 Splitting . . . . .	16
3.9 Chemical Reaction Completion and Sensor Constraints . . . . .	17
3.10 Interconnections . . . . .	17
3.11 Sinks . . . . .	18
4. ANALYSIS OF THE ALGORITHM . . . . .	20
4.1 Optimality Analysis of the Greedy Algorithm . . . . .	20
4.2 System Deadlock . . . . .	23
4.3 Execution Time of the Algorithm . . . . .	24

5. SIMULATION RESULTS . . . . .	26
5.1 Single Mixer in Dual Ring Layout . . . . .	26
5.2 Multiple Mixers and Branched Chain Reactions . . . . .	27
5.3 Performance Evaluation of Phase Assignment . . . . .	28
5.4 Continuous Mode Reactions . . . . .	29
5.5 Comparison of Dual and Synchronous Ring Layouts . . . . .	29
6. HARDWARE IMPLEMENTATION . . . . .	31
6.1 Hardware Interface Design . . . . .	31
6.2 DMFS Control Electronics Setup . . . . .	31
6.3 DMFS Chip Fabrication . . . . .	33
6.4 Design of Layout for Synthesis of Heparin . . . . .	35
7. CONCLUSIONS AND FUTURE WORK . . . . .	38
REFERENCES . . . . .	38

## LIST OF FIGURES

1.1	Droplets on an electrowetting array (side and top views). The droplets are in a medium (usually oil or air) between two glass plates. The gray and white droplets represent the same droplet in initial and final positions. A droplet moves to a neighboring activated electrode which is turned off when the droplet has completed its motion. Based on [18].	3
2.1	Dual ring layout with bus-phase addressing: There are four phases for the outer ring, three for the inner ring, seven for the mixer, and two for each of the interconnections. Within each ring, the phases are allocated among the electrodes in cyclic order. Thus, every fourth electrode in the outer ring has the same phase and every third electrode in the inner ring has the same phase. Based on [21]. . . . .	7
2.2	Synchronous ring layout with bus-phase addressing: There are four phases for all outer rings, seven for all mixers, and three for each of the interconnections. All outer rings are in phase with each other and so are the mixers. . . . .	8
3.1	Example of a chain reaction with four stages. Each stage produces one of the reactants for the next stage. $C$ , $E$ , $G$ are intermediate products and $I$ is the final product. . . . .	11
3.2	Example of a branched chain reaction (PCR analysis graph [19]): Two three-stage chains merge to form a single final product. . . . .	11
4.1	The three possibilities when the greedy algorithm will schedule the droplet pair $(A1, A2)$ before $(B1, B2)$ , i.e., when $d_{A2} < d_{B2}$ . . . . .	20
5.1	Dual ring layout with bus-phase addressing used in our simulations. . .	26
5.2	Synchronous ring layout with bus-phase addressing used for our simulations. The reservoirs for any two reactants forming a compatible pair and the corresponding product are all attached to the same unit to reduce transportation time. Thus, the reservoirs for $A$ , $B$ , and $P$ are all attached to the same outer ring. . . . .	30
6.1	A logical representation of the relationship between the algorithm, hardware interface, and the DMFS chip. . . . .	31
6.2	Hardware interface . . . . .	32
6.3	Electronic setup for manual activation of electrodes. . . . .	33

6.4	A directly addressable DMFS chip fabricated at RPI. . . . .	34
6.5	Chip fabrication process. . . . .	35
6.6	Simplified diagram of heparin synthesis. <i>E1</i> , <i>E2</i> , <i>E3</i> , and <i>E4</i> represent the enzymes that modify the original Streptavidin beads <i>B</i> into <i>B1</i> , <i>B2</i> , <i>B3</i> , and finally <i>H</i> where <i>H</i> stands for the final product <i>heparin</i> . Heparin is then bound to a fluorescent protein <i>FP</i> for easy visualization. <i>H-FP</i> represents heparin bounded to the fluorescent protein. . . . .	36
6.7	The starting unit of the layout for heparin synthesis. <i>E1</i> stands for the first enzyme and <i>B</i> represents magnetic beads in solution. 600 nm Streptavidin beads will be used for heparin synthesis. . . . .	36
6.8	The last unit of the layout for heparin synthesis. <i>FP</i> stands for fluorescent protein and <i>Final</i> represents the final product obtained. . . . .	37
6.9	The layout formed by concatenating units together. A chain reaction can be carried out on this layout with each stage of the reaction occurring on a different unit. . . . .	37

## ACKNOWLEDGMENT

This work was supported in part by NSF under Award No. IIS-0093233, Award No. IIS-0541224, Award No. IIS-0713517, Award No. CNS-0709099, and Award No. CBET-0730817. I would like to thank Eric Griffith for early conversations on this topic and Nilanjan Chakraborty for giving some excellent comments on the work. I am grateful to Prof. Aaron Wheeler and his group, particularly Vivienne Luk and Mohamed Abdelgawad, University of Toronto for working with us on chip fabrication and control electronics. I also extend my thanks to Jeff Martin for many useful discussions on layout designs and electronic equipment setup, and for making all the chemistry involved simple and interesting for me. Last but not the least, I would like to thank my advisor, Dr. Srinivas Akella, for his constant support and guidance, and my colleague, Lingzhi Luo, for many useful insights into the work.

## ABSTRACT

Digital microfluidic systems (DMFS) are a new class of lab-on-a-chip systems for biochemical analysis. A DMFS uses electrowetting to manipulate discrete droplets on a planar array of electrodes. The chemical analysis is performed by repeatedly moving, mixing, and splitting droplets on the electrodes. In this thesis, we present an algorithm for coordinating droplet movement in batch mode operations on DMFS layouts, particularly ring layouts, with bus-phase addressing. In bus-phase systems, individual electrodes are not directly addressable, instead a set of electrodes are all controlled by the same signal. Though this hardware design simplifies chip fabrication, it increases the complexity of routing droplets. The presented algorithm uses the structure of ring layouts to perform droplet collision detection and avoidance, and to generate electrode activations. Droplet injection and mixing operations are scheduled in a greedy manner. The algorithm allows multiple independent and chain reactions to take place simultaneously on the chip and also addresses sensor constraints under which droplets need to visit sensor locations for specified amounts of time. This algorithm is scalable to different number of reactions within a limit that depends on the size of the layout, placement of sources, and number of phases used. Deadlock scenarios, that give an insight into the performance of the algorithm for continuous mode operations, have been identified. We present simulation results using our algorithm to coordinate droplet movement for example analyses on two kinds of ring layouts: dual and synchronous. We also present performance evaluations of the layouts with different number of mixers and different phase assignments. We also present our preliminary work towards interfacing our algorithm with DMFS chips designed and fabricated at RPI.

# 1. INTRODUCTION

## 1.1 Digital Microfluidic Systems

Lab-on-a-chip systems based on digital microfluidic technology have recently generated a lot of interest in the field of biochemical analysis. Digital microfluidic systems (DMFS) manipulate discrete nanoliter-sized droplets on a planar array of electrodes. These systems can be used for rapid automated biochemical analysis, thus impacting a wide variety of applications including biological research, genetic analysis, and biochemical sensing. The biochemical analysis is performed by repeatedly moving, mixing, and splitting droplets on the array. DMFS technology offers scalability, programmability, reconfigurability, and power reduction, and enables analysis of intermediate product droplets. These miniature systems drastically reduce the size of the equipment and the amounts of reagents used for the analysis. However, the DMFS systems currently in use are often programmed manually which greatly limits the scope of this technology, particularly when the number of droplets is large. Therefore, our goal is to design algorithms and computational tools for the automated scheduling and routing of droplets in these systems.

Our focus in this thesis is on DMFS systems that consist of ring layouts with bus-phase addressing [21]. In *bus-phase systems*, each electrode is not directly addressable. Instead, a set of electrodes are controlled by the same signal and are said to have the same *phase*. This design makes fabrication easier and minimizes the number of electrical contacts. However, the complexity of droplet routing goes up significantly because a bus-phase system requires operations to be synchronized and imposes constraints on the parallelism achievable in the analysis. *Ring layouts*, described in detail in Chapter 2, consist of outer and inner rings for transport, mixers, interconnections, and reservoirs. Ring layouts with bus-phase addressing have been used earlier to demonstrate droplet manipulation and pipelined glucose assays<sup>1</sup> [21]. We are not aware of any prior algorithms for the automated control of droplets in

---

<sup>1</sup>Example videos of droplet manipulation on a ring layout may be seen at <http://www.rsc.org/suppdata/lc/b4/b403341h/>.



these systems.

We present an approach to completely automate batch mode operations on ring layouts. For batch mode, we take one droplet each of all reactants to produce one droplet each of all final products. Droplet routes are dynamically chosen and the same set of electrodes is shared among all droplets for transport, mixing, and chemical reaction. The structure of ring layouts is used to perform collision detection and avoidance, and to generate electrode activations. Droplet injection and mixing operations are scheduled in a greedy manner. The algorithm can be used to evaluate the performance of a layout with different phase assignments to select the best one. Once the phase assignment for a layout is done at the fabrication stage, different reactions can be carried out on the same layout without changing the phase assignment. The algorithm scales with the array size; it can handle a larger number of droplets on larger layouts.

## 1.2 Related Work

Almost all current lab-on-a-chip systems use continuous flow microfluidics (for example, [17], [5]). In addition to needing moving parts such as microvalves and micropumps, such devices can perform only one (or a very small number of) pre-specified chemical analyses since fluid flow occurs in fixed channels and are therefore not reconfigurable. Consequently, these devices lack the ability to change analyses in response to intermediate analysis results.

**Digital Microfluidic Systems:** There are two primary methods of actuation in a DMFS: electrowetting [18], where the surface tension of droplets is modulated by a voltage, and dielectrophoresis [23], where a nonuniform electric field causes droplet motion. Pollack, Fair, and Shenderov [18] first demonstrated manipulation of discrete microdroplets by electrowetting-based actuation. Fair et al. [6] described experiments on injection, dispensing, dilution, and mixing of samples in an electrowetting DMFS. Cho, Moon, and Kim [3] demonstrated creating, merging, splitting, and move operations using electrodes covered with dielectrics in an air environment. Paik, Pamula, and Fair [16] studied the effects of droplet aspect ratios and mixing strategies on the rate of droplet mixing. Gong, Fan, and Kim [9] devel-

oped a portable digital microfluidics lab-on-chip platform using electrowetting on dielectrics. They used a time-multiplexed control scheme to control droplets with limited row-column addressing [7].

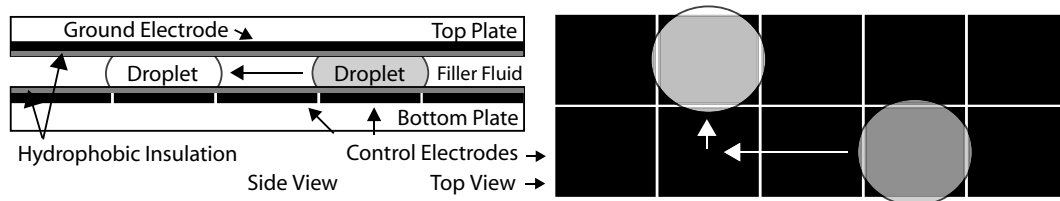


**Figure 1.1: Droplets on an electrowetting array (side and top views).** The droplets are in a medium (usually oil or air) between two glass plates. The gray and white droplets represent the same droplet in initial and final positions. A droplet moves to a neighboring activated electrode which is turned off when the droplet has completed its motion. Based on [18].

Gong and Kim [10] recently developed a directly addressable 2D digital microfluidic system by using multi-layer printed circuit board technology. Jones et al. [13] demonstrated dielectrophoresis based liquid actuation and nanodroplet formation. Gascoyne et al. [8] developed a dielectrophoresis-based chip to move droplets and cells, and Manaresi et al. [15] developed a dielectrophoretic chip capable of manipulating over 10,000 living cells. Recent DMFS research has focused on applications of digital microfluidic chips. Srinivasan et al. [20] demonstrated the use of a DMFS as a biosensor for glucose, lactate, glutamate and pyruvate assays, and for clinical diagnostics on human whole blood, plasma, serum, urine, saliva, sweat, and tears [21]. Pollack et al. [19] demonstrated the use of electrowetting-based microfluidics for real-time polymerase chain reaction (PCR) applications. Wheeler et al. [25] demonstrate an electrowetting-based DMFS for high throughput analysis of proteins by matrix-assisted laser desorption/ionization mass spectrometry.

Despite these rapid advances in digital microfluidic hardware technologies, there is a relative lack of algorithms for automated coordination and control of droplets on DMFS chips. The existing algorithms for automated control of droplets on DMFS platforms typically assume electrodes to be individually addressable; none are designed for bus-phase systems. Ding, Chakrabarty, and Fair [4] described an architectural design and optimization methodology for scheduling biochemical anal-

yses. They identified a basic set of droplet operations and used an integer linear programming formulation to minimize completion time. Here droplet paths and areas on the array for storage, mixing and splitting operations must be predefined by the user. Bohringer [1,2] used limited row-column addressing and pointed out that each droplet in a DMFS can be viewed as a simple robot that moves on a 4-connected array. He outlined an A\* search approach for moving droplets from start to goal locations in prioritized order. However in this approach as well, the locations for all droplet operations are fixed and must be defined by the user. Su and Chakrabarty [22] proposed architectural-level VLSI synthesis techniques for digital microfluidics-based biochips, and described integer programming and heuristic formulations to schedule assay operations, prior to geometry-level synthesis (i.e., without location instantiation on the array). Griffith and Akella [11] developed layout designs and routing algorithms for arrays with direct addressing that can deal with a large number of droplets. Griffith, Akella, and Goldberg [12] presented polynomial-time algorithms for coordinating droplet movement on arrays with limited row-column addressing. Xu and Chakrabarty [26] suggested a droplet-trace-based method for array partitioning and phase assignment in a pin-constrained layout, i.e. a layout where the number of control signals is less than the number of electrodes. Here the droplet routes must be known beforehand and separate areas on the array are reserved exclusively for different droplets.

All these algorithms have either been designed for DMFS with direct addressing or they do not take advantage of the reconfigurability of these systems. Our algorithm completely automates droplet manipulation on ring layouts with bus-phase addressing. It is scalable to different number of reactions on different configurations of ring layouts.

## 2. RING LAYOUTS WITH BUS-PHASE ADDRESSING

The algorithm has been designed for a particular class of DMFS layouts: ring layouts with bus-phase addressing [21]. The five components of a ring layout (Fig. 2.1) are as follows:

1. **Reservoir:** All sources from which reactants are introduced into the DMFS and all sinks to which product and waste droplets are sent, are classified as reservoirs. Each reservoir has a storage area and a neck. The neck facilitates droplet movement between the storage area and the rest of the layout.
2. **Outer ring:** It is a planar ring of electrodes with a fixed number of phases allotted to its electrodes in a cyclic order. In Fig. 2.1, four phases 1, 2, 3, 4 have been assigned to the outer ring. All reservoirs are directly connected to the outer ring.
3. **Mixer:** All operations involving mixing and splitting of droplets happen in the mixer. Mixing refers to the physical merging of two droplets that are supposed to react with each other and splitting refers to the formation of two droplets from the merged droplet. The mixer is directly connected to the outer ring. Seven distinct phases are required for the mixer. In Fig. 2.1, phases 5, 6, 7, 8, 9, 10, 11 have been assigned to the mixer.
4. **Interconnection:** It connects two rings together and allows transport between them. Each electrode in an interconnection is independently addressable. In Fig. 2.1, each interconnection has two electrodes and phases 15, 16 and 17, 18 have been assigned to the left and right interconnections respectively. In Fig. 2.2, each interconnection has three electrodes. Phases 12, 13, 14 have been assigned to the interconnection between the upper two rings.
5. **Inner ring:** An optional component of ring layouts, an inner ring, is a planar ring of electrodes that allows reactions to proceed to completion. A distinct set of phases is allotted to its electrodes in a cyclic order. It may have detection

sites at some of its electrodes to sense the results of reactions. In Fig. 2.1, three phases 12, 13, 14 have been assigned to the inner ring. If the inner ring is absent, the outer ring itself can be used for completion of reaction and sensing requirements.

## 2.1 Dual Ring Layout

We call a ring layout with both outer and inner rings a *dual ring layout*. This hardware architecture has been used earlier for pipelined glucose assays [21]. A useful modification that can be made to this layout is the addition of more mixers and inner rings to allow more reactions to occur in parallel. However, with every additional mixer, the number of phases required increases by seven here.

## 2.2 Synchronous Ring Layout

A different architecture of bus-phased ring layouts has multiple *units*, each consisting of an outer ring and a mixer. All outer rings are *synchronous*, i.e., they have the same phase assignment. All mixers are synchronous too. We call this kind of layout shown in Fig. 2.2 a *synchronous ring layout*<sup>2</sup>. Some advantages of this layout are:

1. Adding more units to the layout increases the number of phases required by a very small number because only the new interconnections require new phases.
2. This layout can be very useful for multiple independent reactions as they require multiple mixers. By arranging the reservoirs carefully, each independent reaction can be carried out in one unit of its own, thus being completely unaffected by other reactions occurring in parallel on the chip.
3. This design is highly scalable as additional units can just be added to the existing layout if more reactions need to be carried out on the chip.

---

<sup>2</sup>This layout is inspired by layouts designed by Eric J. Griffith.

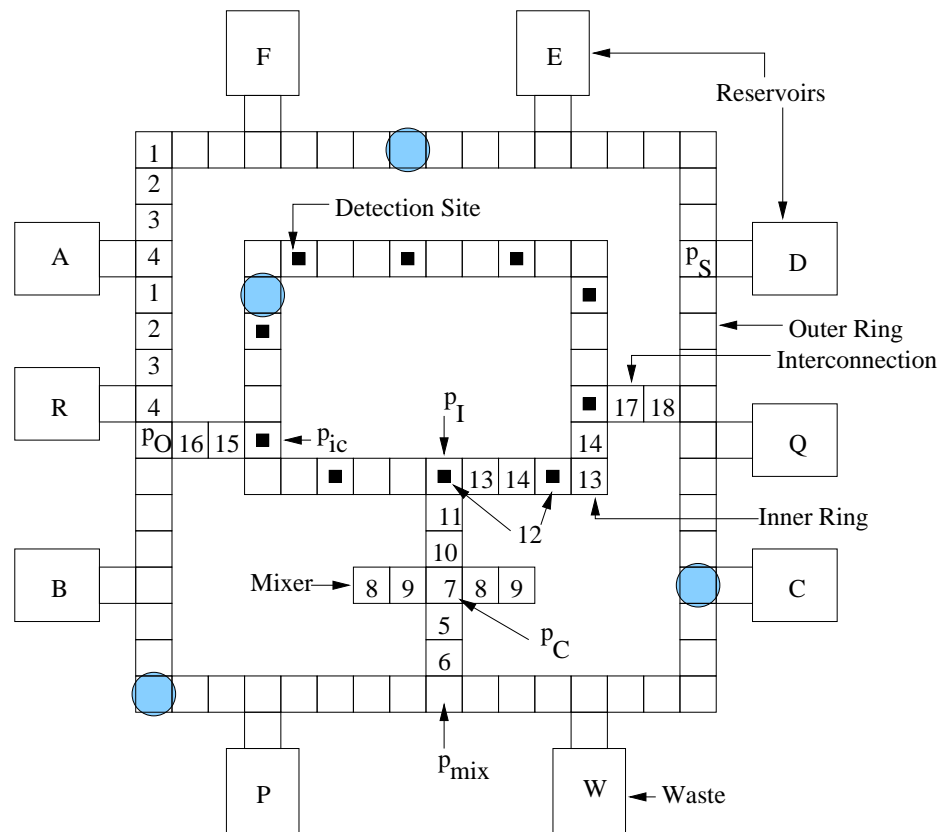


Figure 2.1: Dual ring layout with bus-phase addressing: There are four phases for the outer ring, three for the inner ring, seven for the mixer, and two for each of the interconnections. Within each ring, the phases are allocated among the electrodes in cyclic order. Thus, every fourth electrode in the outer ring has the same phase and every third electrode in the inner ring has the same phase. Based on [21].

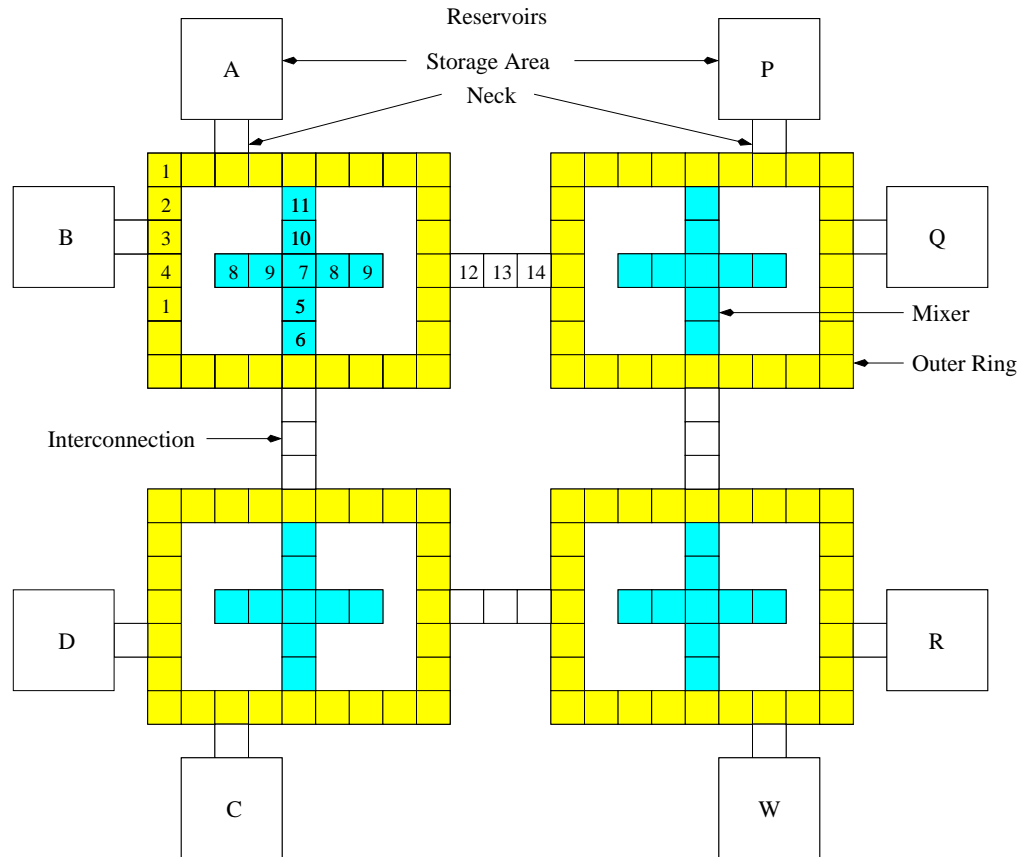


Figure 2.2: Synchronous ring layout with bus-phase addressing: There are four phases for all outer rings, seven for all mixers, and three for each of the interconnections. All outer rings are in phase with each other and so are the mixers.

## 3. THE ALGORITHM

### 3.1 Problem Statement

**Goal:** Given a ring layout with bus-phase addressing, and a set of reactions, schedule and route the droplets so as to complete the chemical analysis, without any inadvertent mixing. Starting with one droplet of each reactant, a droplet of each final product must be produced with all timing constraints on mixing, reacting, and sensing satisfied.

**Input:** Number of electrodes in the rings, locations of mixers, rings, interconnections, and reservoirs, reagents stored in each reservoir, electrode phase assignments, reactions to be carried out, and mixing, reaction, and sensing times.

**Output:** Electrode activation schedule to coordinate droplet routing and to sense results of reactions.

### 3.2 Applicability of the Algorithm to Different Layouts

The algorithm has been successfully tested on the two kinds of ring layouts described in Chapter 2. Further it can also work for many other ring layouts with similar features. Some characteristic features of the ring layouts to which this algorithm is applicable are:

1. The reservoirs must be attached directly to the outer ring.
2. Phases must be assigned to electrodes in any ring in a cyclic order.
3. Any two rings must be connected by an interconnection consisting of two or more independently addressable electrodes.
4. Any mixer should be directly attached to a ring on any two of its opposite sides.
5. Except the mixer electrodes, if an electrode  $e_i$  has more than two neighbors, only two of them can belong to the same component as  $e_i$  because the algorithm is designed to take care of three-way intersections only.

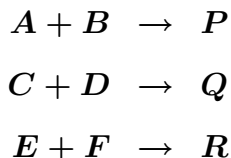


If the above constraints on the layout are satisfied, the algorithm will be able to perform droplet scheduling, routing, collision detection, and collision avoidance correctly.

### 3.3 Applicability of the Algorithm to Different Reactions

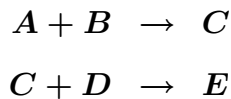
The algorithm is applicable to two classes of reactions listed below. Any combination of these two types of reactions occurring in parallel on the same layout can be controlled by the algorithm.

1. **Independent reactions:** Independent reactions are those that form no intermediate products. Each independent reaction is assumed to consist of two reactants and one product. An example set of independent reactions is:



where  $A$ ,  $B$ ,  $C$ ,  $D$ ,  $E$ , and  $F$  are chemical reagents to be mixed and  $P$ ,  $Q$ ,  $R$  are the final products. A possible assignment of reservoirs for this example is shown in Fig. 2.1. We will call a pair of droplets of types that are supposed to react with each other a *compatible pair* of droplets. Thus,  $(A, B)$  form a compatible pair, and we have a total of three compatible pairs in the above example.

2. **Chain reactions:** Chain reactions consist of a series of reactions, each reaction defining a *stage*, whose products are used as reactants for the next stage. Each stage of a chain reaction is assumed to consist of two reactants and one product. Chain reactions can be *linear* or *branched*. An example of a *linear chain reaction*, i.e., a chain reaction with a single chain (Fig. 3.1) is:





where  $C$ ,  $E$ ,  $G$  are intermediate products and  $I$  is the final product. For the example above, stage 1 refers to the first reaction in the chain and stage 4 refers to the last reaction. *Branched chain reactions* are reactions where multiple chains merge to form a single final product. An example of such a reaction is the polymerase chain reaction (PCR) for DNA sequence analysis [19] (Fig. 3.2).

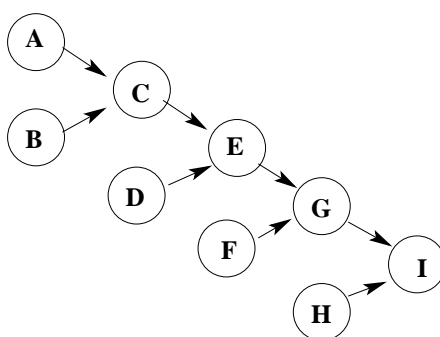


**Figure 3.1:** Example of a chain reaction with four stages. Each stage produces one of the reactants for the next stage.  $C$ ,  $E$ ,  $G$  are intermediate products and  $I$  is the final product.

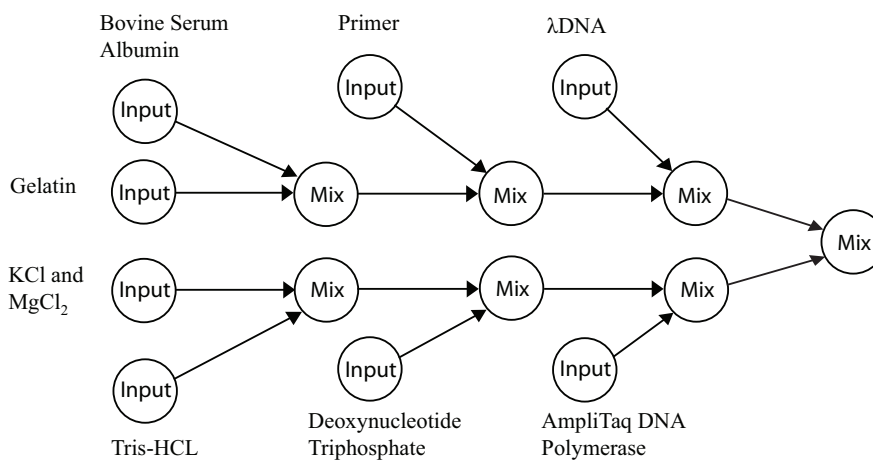


**Figure 3.2:** Example of a branched chain reaction (PCR analysis graph [19]): Two three-stage chains merge to form a single final product.

### 3.4 Overview

The algorithm generates proper electrode activations for all steps in a biochemical analysis such that there are no unwanted droplet movements or mixing throughout the analysis, and all timing constraints are satisfied. Reagent transport and droplet mixing occur on the same shared set of electrodes. Since multiple electrodes are controlled by the same signal, activation of an electrode with a particular phase can result in droplet movements at all other electrodes with the same phase. Hence, the complexity of preventing undesired mixing between droplets is greater for bus-phase systems. The sequence of steps to be carried out for any reaction, the electrode activations for which are automated by the algorithm, is essentially the same:

1. Introduce the droplets into the system from sources.
2. Merge compatible pairs of droplets in the mixer. Move the merged droplet multiple times in the mixer for the input mixing time,  $t_{mix}$ , to ensure uniformity in composition inside the droplet.
3. Split the mixed droplet to form two regular-sized product droplets. Send one of them for completion of the chemical reaction and the other to the waste outlet.
4. Retain the product droplet in the inner/outer ring for the prescribed reaction time,  $t_{react}$ , to allow the chemical reaction to complete.
5. For any sensing requirements, sense the product droplet for the input sensing time,  $t_{sense}$ .
6. Send final products to their respective sinks.

Let the current position of droplet  $i$  be denoted by  $\mathbf{p}_i$  and that of an electrode  $e$  by  $\mathbf{p}_e$ . Specifically, let us denote entry to the mixer by  $\mathbf{p}_{mix}$ , the central electrode of the mixer by  $\mathbf{p}_C$ , an electrode adjacent to any source or sink by  $\mathbf{p}_S$ , entry to the inner ring by  $\mathbf{p}_I$ , and any entry to the outer ring from the inner ring by  $\mathbf{p}_O$ . We will consider the anticlockwise direction as positive. So,  $\mathbf{p}_{e-n}$  refers to the electrode that

is  $n$  electrodes before the electrode  $e$  in the same ring. All current droplet positions are calculated and updated by the algorithm after every clock cycle so that the droplet positions are always known globally. We will now list the assumptions we make and then describe in detail how each of the operations like droplet dispensing, routing, mixing, and splitting is handled by the algorithm.

### 3.5 Assumptions

1. The mixer is used only for physical mixing of droplets. It can be entered from both the rings (if inner ring is present) for chain reactions but only from the outer ring for independent reactions.
2. Any new droplet formed in the mixer that is neither a final product nor an intermediate product is labeled a waste droplet. Such droplets exit only to the outer ring from the mixer and are directed to the waste outlet.
3. Completion of chemical reaction and sensing of droplets takes place in the inner ring for dual ring layouts and in the outer ring for synchronous ring layouts. The inner ring can be entered only from the mixer.
4. In all the rings, droplets move in the anticlockwise direction only and the rings may be deactivated, i.e., paused completely, when desired. This means that none of the phases in a ring are activated, thus stopping all droplet motion in that ring. When they are reactivated, they resume from current phases.

### 3.6 Injection from Sources

For chain reactions, we assume the introduced droplets have the correct concentration. Before the droplet is introduced into the outer ring, the source electrodes are ON, neck electrode is OFF and  $p_S$  may be ON or OFF. To introduce the droplet, use Algorithm 1. The sources may or may not be connected to different phases of the outer ring. If the neck electrodes of two sources,  $S$  and  $S'$ , connected to the same phase  $i$  of the outer ring have the same phase  $j$ , then to introduce a droplet from  $S$ ,  $j$  will have to be activated followed by  $i$ . This will lead to a droplet from

$S'$  also getting introduced into the outer ring even though it was not planned. To avoid this, the neck electrode of each source should have a unique phase.

---

**Algorithm 1:** Droplet injection from sources

---

- 1 **if**  $\mathbf{p}_{S-2}$  is empty when  $\mathbf{p}_{S-2}$  is activated **then**
  - 2     Activate neck electrode and turn off source electrodes simultaneously when  $\mathbf{p}_{S-1}$  turns on.
  - 3     Switch off neck electrode when  $\mathbf{p}_S$  turns on so that one droplet is introduced into the outer ring.
  - 4     Activate source electrodes again.
  - 5 **else** Go to step 1.
- 

### 3.7 Mixing

For the dual ring layout and each unit of the synchronous ring layout, we employ a greedy algorithm to introduce droplets into a mixer. Though this may not give us a globally optimum solution in all cases, it is simple to implement and incurs low computational overhead. The global optimum depends on a number of factors like the mixing times and time taken by the split droplets to leave the mixer. The second factor in turn depends on availability of space in the outer and inner rings, which changes dynamically.

The greedy scheduling algorithm has been outlined in Algorithm 2. The expression in line 4 of this algorithm calculates for every compatible pair of droplets, the distance of the droplet which is farther away from the mixer. The pair of droplets for which this distance is the least can be brought to the mixer in the least number of clock cycles. Therefore, that pair of droplets is chosen to be sent to the mixer. Suppose the pair  $(A, B)$  are chosen. Then, the minimum number of clock cycles required is  $\mathbf{max}(d(\mathbf{p}_A, \mathbf{p}_{mix}), d(\mathbf{p}_B, \mathbf{p}_{mix}))$ . A droplet's motion is affected by interference by other droplet motions and electrode activations. For example, the outer ring may need to be paused to allow a droplet to enter a sink. So, the number of actual clock cycles may be more than the number of theoretical minimum clock cycles calculated. For synchronous ring layouts, if the two droplets of a compatible pair are present in the outer rings of two different units, then an empty mixer in any one of these units is chosen as the destination for the pair.

---

**Algorithm 2:** Scheduler for mixing
 

---

```

1 min ← number of electrodes in outer ring
2 pair ←  $\phi$ 
3 for every clock cycle do
4   foreach compatible pair  $(X, Y)$  in the outer ring do
5     dist ←  $\max\{d(\mathbf{p}_X, \mathbf{p}_{mix}), d(\mathbf{p}_Y, \mathbf{p}_{mix})\}$ 
        //  $d(\mathbf{u}, \mathbf{v}) = 1 + \text{number of electrodes between the two positions}$ 
        //  $\mathbf{u}$  and  $\mathbf{v}$ 
6     if dist < min then pair ←  $(X, Y)$ 
7   endfch
8   Set  $\mathbf{p}_{mix}$  as destination of pair.
9 end

```

---

The pair destined for a mixer can enter the correct mixer using Algorithm 3. The representative phases given in the algorithm refer to Fig. 2.1. This procedure will have to be used twice, once for each droplet in the pair. In the case of chain reactions occurring on a dual ring layout, the intermediate droplets can enter the mixer from the inner ring itself, once they have reacted completely. Lines 10 – 18 of Algorithm 3 take this possibility into account.

However, it is possible that the outer ring is fully occupied and none of the droplets in the outer ring have to be sent to a sink, as a result of which a compatible pair cannot be formed till a new droplet is introduced in the outer ring. In this case, whichever droplet with mixer as the destination reaches  $\mathbf{p}_{mix}$  first is taken in by the mixer. Now that the mixer has one droplet, every time a droplet with mixer as the destination reaches  $\mathbf{p}_{mix}$ , a check is performed to see if it is compatible with the droplet already present in the mixer. If it is, the droplet is sent to the mixer otherwise it is moved further in the outer ring itself.

Once both types of droplets are present in the mixer, we look up the required physical mixing time,  $t_{mix}$ , for the pair and repeat the following sequence of electrode activations for  $t_{mix}$  clock cycles to enable mixing to occur:  $8 \rightarrow 9 \rightarrow 8 \rightarrow 7 \rightarrow 9 \rightarrow 8 \rightarrow 9 \rightarrow 7$ . If at the end of  $t_{mix}$  cycles, the merged droplet is not at  $\mathbf{p}_C$ , continue with the above sequence of activations till the droplet reaches  $\mathbf{p}_C$ .

It is important to note that Algorithms 2 and 3 can be carried out exactly the same way for a ring layout with multiple mixers too because the algorithm depends

---

**Algorithm 3:** Taking a droplet into a mixer
 

---

```

1 foreach droplet reaching  $\mathbf{p}_{mix}$  do
2   if its destination is  $\mathbf{p}_{mix}$  then
3     Pause outer ring and activate phase 6 so that the droplet enters
       mixer.
4     if no droplet present at  $\mathbf{p}_C$  then
5       Activate phase 5 and restart the outer ring simultaneously.
6     else Activate phase 10 and go to step 4.
7     Activate phase 7 so that the droplet reaches  $\mathbf{p}_C$ .
8   end
9 endfch
10 foreach droplet reaching  $\mathbf{p}_I$  do
11   if its destination is  $\mathbf{p}_I$  then
12     Pause inner ring and activate phase 11.
13     if no droplet present at  $\mathbf{p}_C$  then
14       Activate phase 10 and restart the inner ring simultaneously.
15     else Activate phase 5 and go to step 13.
16     Activate phase 7 so that the droplet reaches  $\mathbf{p}_C$ .
17   end
18 endfch

```

---

only on  $\mathbf{p}_{mix}$ ,  $\mathbf{p}_I$ , and phases of the mixer. Therefore, each mixer can use these algorithms with its own values of  $\mathbf{p}_{mix}$ ,  $\mathbf{p}_I$ , and phases to look for the closest pair of compatible pair of droplets, take them in using correct electrode activation sequence and mix them for the prescribed mixing time.

### 3.8 Splitting

The merged droplet is double the volume of regular droplets. It can be split by activating the two electrodes on its either side simultaneously, i.e., by turning off phase 7 and activating phases 5 and 10 simultaneously (Fig. 2.1). Splitting results in two regular-sized droplets, one on phase 5 and the other on phase 10. Note that if  $\mathbf{p}_I$  is at phase  $\mathbf{j}$ , we can introduce a droplet at  $\mathbf{p}_I$  only when phase  $\mathbf{j}$  is activated. So, if a droplet is to be sent to the inner ring, it is first checked if  $\mathbf{p}_{I-2}$  is empty when it is activated because if there is already a droplet at  $\mathbf{p}_{I-2}$ , it would reach  $\mathbf{p}_I$  when phase  $\mathbf{j}$  is activated and mix with the droplet from the mixer. If both split droplets have to be sent to the inner ring, use Algorithm 4. If one of the split droplets has to

be sent to the waste outlet via the outer ring, then use Algorithm 5. Again, these procedures can be used for a ring layout with multiple mixers and multiple inner rings because they depend only on  $\mathbf{p}_{mix}$ ,  $\mathbf{p}_I$ , and phases of the mixer. Therefore, each mixer and inner ring will need to use a distinct set of phases and then can use these procedures with its own values of  $\mathbf{p}_{mix}$ ,  $\mathbf{p}_I$ , and phases.

### 3.9 Chemical Reaction Completion and Sensor Constraints

If some sensor constraints have been specified by the user, optical detection sites are located in the inner or outer ring to fulfill them. For example, the droplet may be required to stay on a detection site for a prescribed number of clock cycles, say  $t_{sense}$ , after the completion of the chemical reaction. In Fig. 2.1, every inner ring electrode with phase 12 is a detection site. Algorithm 6 allows the reactions to complete and takes the sensor constraints into account accordingly for dual ring layouts. The algorithm for synchronous ring layouts is the same except that the final product droplet stays in the outer ring of its unit till the chemical reaction reaches completion. After that, if the corresponding sink is attached to some other unit, the droplet is guided to that unit via one of the interconnections attached to its current unit.

### 3.10 Interconnections

Each interconnection requires distinct phases for its electrodes. If the same set of phases is used for two interconnections  $IC1$  and  $IC2$ , then unwanted droplet movement can occur around  $IC2$  when any phase of  $IC1$  is activated. Suppose phases 15 and 16 are used for one of the interconnections as shown in Fig. 2.1. Let us call the inner ring electrode adjacent to the interconnection  $\mathbf{p}_{ic}$ . Algorithm 7 allows movement of droplets from the inner ring to the outer ring in dual ring layouts. For synchronous ring layouts, the source ring replaces the inner ring, and the destination ring replaces the outer ring in Algorithm 7.



---

**Algorithm 4:** Movement of split droplets out of mixer(a)

---

```

1 Split the merged droplet.
2 while the mixer is not empty do
3   if  $p_{I-2}$  is empty when it is activated then
4     Activate phase 11 when  $p_{I-1}$  is activated so that one of the split
       droplets moves toward the inner ring.
5     Activate phase 7 in the next clock cycle so that the other droplet
       reaches  $p_C$ .
6     Activate phase 10 and switch off phase 11 when phase  $j$  is
       activated so that the first droplet enters the inner ring while the
       second one moves toward it.
7   end
8 end

```

---



---

**Algorithm 5:** Movement of split droplets out of mixer(b)

---

```

1 Split the merged droplet. Perform steps 2 and 5 below simultaneously.
2 if  $p_{I-2}$  is empty when it is activated then
3   Activate phase 11 when  $p_{I-1}$  is activated so that one of the split
       droplets moves toward the inner ring. This droplet would now enter
       the inner ring when phase  $j$  is activated.
4 else Go to step 2.
5 if  $p_{mix-2}$  is empty when it is activated then
6   Activate phase 6 when  $p_{mix-1}$  is activated so that the waste droplet
       moves toward the outer ring. This droplet would now enter the outer
       ring when electrode  $p_{mix}$  is activated.
7 else Go to step 5.

```

---

### 3.11 Sinks

As for sources, multiple sinks may be connected to the same phase of the outer ring and so, the neck electrode of each sink should have a unique phase. To send a droplet to sink **S1**, mark  $p_{S1}$  as the droplet's destination when it has undergone complete chemical reaction and is present in the outer ring, and use Algorithm 8.

---

**Algorithm 6:** Chemical reaction and droplet sensing
 

---

```

1 Move a droplet in the inner ring for  $t_{react}$  clock cycles so that the
  chemical reaction is completed.
2 if no sensor constraints specified then Go to step 9.
3 else
4   if the droplet is not on a detection site then
5     move it to the closest detection site.
6   Pause the inner ring for  $t_{sense}$  clock cycles.
7   Restart the inner ring.
8 end
9 if the droplet is a final product then
10  Calculate the location of the interconnection closest to the
    corresponding sink and set it as the droplet's destination.
11 else Set  $p_I$  as the droplet's destination to resend it to the mixer.

```

---



---

**Algorithm 7:** Movement between rings
 

---

```

1 foreach droplet reaching  $p_{ic}$  do
2   if its destination is  $p_{ic}$  then
3     Pause inner ring.
4     if  $p_{O-3}$  is empty when it is activated then
5       Activate phase 15 and restart the inner ring when electrode
         $p_{O-2}$  is turned on.
6       Switch off phase 15 and activate 16 when electrode  $p_{O-1}$  is on.
7       Turn off 16 when electrode  $p_O$  is activated so that the droplet
        moves to the outer ring.
8     end
9   end
10 endfch

```

---



---

**Algorithm 8:** Droplet removal from DMFS array
 

---

```

1 foreach droplet reaching  $p_{S1}$  do
2   if its destination is  $p_{S1}$  then
3     Pause outer ring and activate the neck electrode of S1 so that the
      droplet enters S1.
4     Turn off neck electrode and switch on sink electrodes. Then,
      restart the outer ring.
5   end
6 endfch

```

---

## 4. ANALYSIS OF THE ALGORITHM

### 4.1 Optimality Analysis of the Greedy Algorithm

To better understand the performance of our greedy algorithm for scheduling mixing operations (Section 3.7), we present a preliminary analysis for two reactions on the dual ring layout. Consider two compatible droplet pairs,  $(\mathbf{A1}, \mathbf{A2})$  and  $(\mathbf{B1}, \mathbf{B2})$ . Let  $\mathbf{A1}$  and  $\mathbf{B1}$  be closer to  $\mathbf{p}_{mix}$  than  $\mathbf{A2}$  and  $\mathbf{B2}$  respectively. For droplet  $i$ , let  $d_i = d(\mathbf{p}_i, \mathbf{p}_{mix})$ . Without loss of generality, let  $d_{A2} < d_{B2}$ . This can happen in three ways as shown in Fig. 4.1.

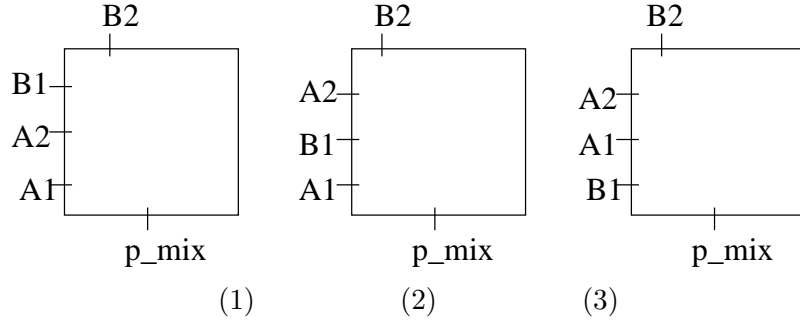


**Figure 4.1:** The three possibilities when the greedy algorithm will schedule the droplet pair  $(\mathbf{A1}, \mathbf{A2})$  before  $(\mathbf{B1}, \mathbf{B2})$ , i.e., when  $d_{A2} < d_{B2}$ .

$d_{A2} < d_{B2}$  means the greedy algorithm,  $\mathbf{G}$ , will always schedule  $(\mathbf{A1}, \mathbf{A2})$  before  $(\mathbf{B1}, \mathbf{B2})$ . Let  $\mathbf{OPT}'$  be a schedule that always schedules  $(\mathbf{B1}, \mathbf{B2})$  before  $(\mathbf{A1}, \mathbf{A2})$ . Let the number of clock cycles required by  $\mathbf{G}$  to complete mixing of both pairs be  $T_G$  and that required by  $\mathbf{OPT}'$  be  $T_{opt'}$ . We will now analyze whether  $\mathbf{G}$  is optimal for the three cases in Fig. 4.1 with zero and finite mixing times.

1.  $t_{mix} = 0$  for both pairs. We show that the greedy solution is always optimal in this case.

**Case 1:**  $d_{A2} < d_{B1}$ . Here,  $\mathbf{G}$  takes  $d_{A2}$  cycles to take  $(\mathbf{A1}, \mathbf{A2})$  in the mixer. By then,  $\mathbf{B2}$  has moved  $d_{A2}$  electrodes closer to  $\mathbf{p}_{mix}$ . So,  $\mathbf{G}$  takes another  $(d_{B2} - d_{A2})$  cycles to take  $(\mathbf{B1}, \mathbf{B2})$  in the mixer. On the other hand,  $\mathbf{OPT}'$  takes  $d_{B2}$  cycles to take  $(\mathbf{B1}, \mathbf{B2})$  in the mixer. By then,  $\mathbf{A2}$  has moved

$(d_{B2} - d_{A2})$  electrodes past  $p_{mix}$ . So,  $\mathbf{G}$  takes another  $n_O - (d_{B2} - d_{A2})$  cycles to take  $(\mathbf{A1}, \mathbf{A2})$  in the mixer. Therefore,

$$\begin{aligned} T_G &= d_{A2} + (d_{B2} - d_{A2}) \\ &= d_{B2} \\ T_{opt'} &= d_{B2} + n_O - (d_{B2} - d_{A2}) \\ &= n_O + d_{A2} \end{aligned}$$

Case 2:  $d_{A2} > d_{B1}$ .

$$\begin{aligned} T_G &= d_{A2} + n_O - (d_{A2} - d_{B1}) \\ &= n_O + d_{B1} \\ T_{opt'} &= d_{B2} + n_O - (d_{B2} - d_{A2}) \\ &= n_O + d_{A2} \end{aligned}$$

Case 3:  $d_{A1} > d_{B1}$ .

$$\begin{aligned} T_G &= d_{A2} + n_O - (d_{A2} - d_{B1}) \\ &= n_O + d_{B1} \\ T_{opt'} &= d_{B2} + n_O - (d_{B2} - d_{A2}) \\ &= n_O + d_{A2} \end{aligned}$$

Thus,  $T_G < T_{opt'}$  whenever  $t_{mix} = 0$  for each pair. As there are only two possible schedules for two droplet pairs out of which  $\mathbf{G}$  is better, it is also the optimal.

2.  $t_{mix} > 0$  for both pairs.

Here, let us assume that  $t_{mix}$  for each pair is sufficiently large so that while it is mixing, the other pair goes past the mixer exactly once. Let  $t_{mix1}$  and  $t_{mix2}$  be the mixing times for the two pairs respectively.

Case 1:  $d_{A2} < d_{B1}$ .

$$\begin{aligned}
T_G &= d_{A2} + t_{mix1} + n_O - (t_{mix1} - (d_{B2} - d_{A2})) \\
&\quad + t_{mix2} \\
&= n_O + d_{B2} + t_{mix2} \\
T_{opt'} &= d_{B2} + t_{mix2} + n_O - (t_{mix2} + d_{B2} - d_{A2}) \\
&\quad + t_{mix1} \\
&= n_O + d_{A2} + t_{mix1}
\end{aligned}$$

Case 2:  $d_{A2} > d_{B1}$ .

$$\begin{aligned}
T_G &= d_{A2} + t_{mix1} + n_O - (t_{mix1} - (d_{B2} - d_{A2})) \\
&\quad + t_{mix2} \\
&= n_O + d_{B2} + t_{mix2} \\
T_{opt'} &= d_{B2} + t_{mix2} + n_O - (t_{mix2} + d_{B2} - d_{A2}) \\
&\quad + t_{mix1} \\
&= n_O + d_{A2} + t_{mix1}
\end{aligned}$$

Case 3:  $d_{A1} > d_{B1}$ .

$$\begin{aligned}
T_G &= d_{A2} + t_{mix1} + n_O - (t_{mix1} - (d_{B2} - d_{A2})) \\
&\quad + t_{mix2} \\
&= n_O + d_{B2} + t_{mix2} \\
T_{opt'} &= d_{B2} + t_{mix2} + n_O - (t_{mix2} + d_{B2} - d_{A2}) \\
&\quad + t_{mix1} \\
&= n_O + d_{A2} + t_{mix1}
\end{aligned}$$

Hence, in this case, whether  $T_G < T_{opt'}$  or not depends on the distance of each compatible pair from the mixer and  $t_{mix}$  for each pair. So,  $\mathbf{G}$  may not always

be the best choice.

## 4.2 System Deadlock

System deadlock means that the system gets stuck in a particular state, preventing any further progress of the biochemical analysis. Here we identify deadlock scenarios for the dual ring layout. Let  $e_o$  and  $e_i$  be the number of electrodes in the outer and the inner ring respectively,  $n_i$  and  $n_{mix}$  the number of droplets in the inner ring and mixer respectively,  $w_{mix}$  the number of waste droplets in the mixer, and  $w_o$  the number of waste or final product droplets in the outer ring.

The key observation in calculating the number of droplets that can cause a deadlock is that the droplets can leave the system only through the outer ring. Therefore, if the outer ring is filled to its capacity but has no waste or final product droplets, and if the mixer has at least one waste droplet that cannot exit to the outer ring, the system reaches a deadlock as none of the droplets from the outer ring can leave the system or enter the mixer. Since the outer ring has four phases, every fourth electrode will have a droplet on it. Thus, the number of droplets in such a case is  $(e_o/4 + n_i + n_{mix})$  where

$$0 \leq n_i \leq e_i/3;$$

$$0 < n_{mix} \leq 2;$$

$$w_o = 0;$$

$$w_{mix} > 0.$$

A deadlock can also occur if both the split droplets must go to the inner ring. In this case, if both the rings are filled to their capacity and the outer ring has no waste or final product droplets, no movement from the inner ring to the outer ring or from the outer ring to the mixer can occur. Since the inner ring has three phases, every third electrode of the inner ring will have a droplet on it. Therefore, the number of droplets in this case is  $(e_o/4 + e_i/3 + n_{mix})$  where

$$0 < n_{mix} \leq 2;$$

$$\begin{aligned} \mathbf{w}_o &= \mathbf{0}; \\ \mathbf{w}_{mix} &= \mathbf{0}. \end{aligned}$$

In Fig. 2.1 ,  $e_o = 60$ ,  $e_i = 30$ , and we treat one of the split droplets as waste. Thus, as few as 16 droplets can cause a deadlock with 15 droplets in the outer ring,  $w_o = 0$ , and a waste droplet in the mixer.

### 4.3 Execution Time of the Algorithm

The execution time of each of the droplet operations is given below. Only Algorithm 2 that handles mixer scheduling is called at every clock cycle. All others are invoked at certain time instants only. However, the sum of all these execution times does not give the *completion time* of the analysis on a given layout because several of these operations occur in parallel on the DMFS array.

1. Droplet injection from sources: This operation as defined in Algorithm 1 is performed at a source only when a droplet has to be introduced from the source into the system. Assuming at least one free spot for the new droplet in the outer ring, the new droplet may have to wait for at most  $e_o$  clock cycles before it can be introduced ( $e_o$  is the number of electrodes in the outer ring). Therefore, this is an  $\mathcal{O}(e_o)$  operation for each source.
2. Mixing scheduler: The scheduler runs Algorithm 2 at every clock cycle. If  $p$  is the number of compatible pairs in the outer ring at any time instant, scheduling takes  $\mathcal{O}(p)$  time for each mixer. If  $m$  is the number of mixers, the scheduling operation is  $\mathcal{O}(mp)$  at every clock cycle.
3. Intake of droplets by a mixer: This operation as defined by Algorithm 3 occurs only when a droplet reaches  $p_{mix}$  or  $p_I$  for some mixer. If  $d_o$  is the number of droplets in the outer ring and  $d_i$  in the inner ring, this operation is  $\mathcal{O}(d_o + d_i)$  for each mixer. This can be simplified to  $\mathcal{O}(md)$  for all mixers.
4. Physical mixing of droplets: This is an  $\mathcal{O}(t_{mix})$  operation for each mixer.

5. Movement of split droplets out of the mixer: This operation as defined by Algorithms 4 and 5 occurs only after splitting occurs inside a mixer. The execution time for these algorithms is equal to the time required to vacate the mixer. Assuming at least one free spot each in the outer ring and the inner ring for the split droplets to take, the split droplets may have to wait for at most  $e_o$  and  $e_i$  clock cycles respectively before they can leave the mixer ( $e_o$  and  $e_i$  are the number of electrodes in the outer ring and the inner ring respectively.). Therefore, this is an  $O(e_o + e_i)$  operation for each mixer.
6. Chemical reaction and sensing: This operation as defined by Algorithm 6 occurs for each droplet that enters the inner ring and is  $O(t_{react} + t_{sense})$  for each droplet in the inner ring.
7. Movement between rings: Algorithm 7 is called whenever a droplet in the inner ring reaches  $p_{ic}$ . Assuming at least one free spot in the outer ring, the inner ring droplet that wants to exit to the outer ring may have to wait for at most  $e_o$  clock cycles before it can exit ( $e_o$  is the number of electrodes in the outer ring). Therefore, this is an  $O(e_o)$  operation for each droplet in the inner ring that has to exit to the outer ring and  $O(1)$  for the droplet that does not have to.
8. Droplet removal from DMFS array: Algorithm 8 is called whenever a droplet in the outer ring reaches  $p_S$  of a sink and is an  $O(1)$  operation irrespective of whether the droplet's destination is that sink or not.



## 5. SIMULATION RESULTS

### 5.1 Single Mixer in Dual Ring Layout

The algorithm has been implemented in C++ and simulated successfully for both independent and chain reactions. We define *completion time* of the analysis as the number of clock cycles required to reach the state when all reactions have been completed, and all product droplets on the array have been sent to the respective sinks or waste outlet, thus leaving no droplet on the array.

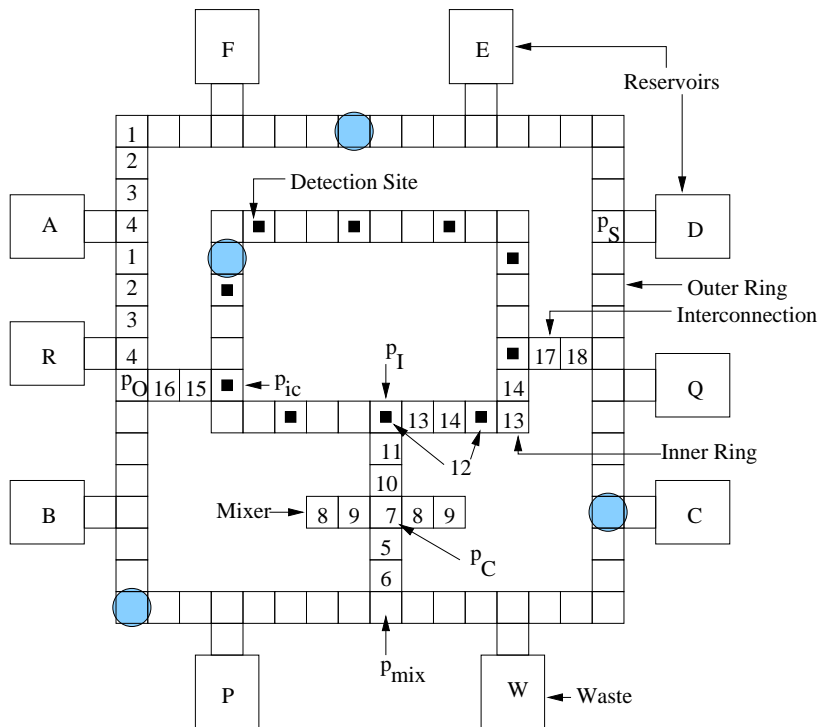


**Figure 5.1: Dual ring layout with bus-phase addressing used in our simulations.**

The simulations referred to in the following results were carried out on a ring layout with  $e_o = 60$ ,  $e_i = 30$ , 1 mixer, 4 phases in the outer ring, and 3 phases in the inner ring (see Fig. 5.1). For an example analysis consisting of three independent reactions with  $t_{mix} = 10$ ,  $t_{react} = 20$ , and no sensor constraints, a completion time of 270 clock cycles was achieved. For a seven-stage chain reaction with  $t_{mix} = 5$ ,  $t_{react} = 20$ , and  $t_{sense} = 5$ , a completion time of 513

clock cycles was achieved. The mixing times used for the simulations have been picked based on the videos showing pipelined glucose assays on a dual ring layout (<http://www.rsc.org/suppdata/lc/b4/b403341h/>) [21]. However, the algorithm is independent of the magnitude of these times.

The algorithm can be optimized for chain reactions by relaxing some of the assumptions. For example, instead of just giving the compatible pairs as input to the algorithm, if the precedence relationship among reactions in the chain is also fed in, the overall transportation time of droplets and the idle time of the mixer is greatly reduced. Also, allowing the intermediate droplets of a chain reaction to enter the mixer from the inner ring itself also reduces the transportation time. The reduction in completion time achieved due to these optimizations has been presented in Table 5.1.

**Table 5.1: Optimizations for Chain Reactions**

Algorithm	Standard assumptions	Define chain structure	Movement from inner ring to mixer
Completion time (clock cycles)	513	460	387

We have simulated example independent and chain reactions operating in batch mode. Animation of a chain reaction with seven stages and sensor constraints has been attached with the paper. In the video, droplets having the same color represent a compatible pair. One of the droplets from each split operation is treated as waste. The gray reservoir is for waste droplets and the dark green reservoir is for the final product. Other animations of independent reactions, chain reactions without sensor constraints, and chain reaction with and without predefined stages can be seen at <http://www.cs.rpi.edu/~sakella/BusedDMFS>.

## 5.2 Multiple Mixers and Branched Chain Reactions

As discussed earlier, the algorithm extends to modified ring layouts with multiple mixers and multiple inner rings as well. This can be important as additional mixers can reduce the completion time for independent reactions and for chain re-

actions, multiple executions of the chain can be done in parallel to obtain multiple droplets of the final product in lesser time. For the example simulation with three independent reactions and a four-based outer ring in a dual ring layout (Fig. 5.1), the completion time changed with the number of mixers as shown in Table 5.2.

**Table 5.2: Completion time reduction with increase in number of mixers**

Number of Mixers	1	2	3	4
Completion Time (clock cycles)	194	154	151	137

We have also performed branched chain reactions, where multiple chains merge to form a single final product, by treating each stage as an independent reaction. In this case also, multiple mixers enable different branches of the chain to execute independently and thus, reduce overall completion time.

### 5.3 Performance Evaluation of Phase Assignment

The algorithm can be used to simulate analyses with different number of phases in the two rings prior to chip fabrication to test which phase assignment would minimize the completion time. The results for this performance evaluation for various number of phases and mixers for the example analyses with three independent reactions on a dual ring layout are given in Table 5.3.

**Table 5.3: Performance evaluation with different phase assignments**

Phases in Outer Ring	Number of Mixers			
	1	2	3	4
3	254	152	150	135
4	194	154	151	137
5	254	157	153	138
6	260	156	156	144

This table suggests that a three-phased outer ring would be the best choice and a six-phased outer ring the worst. It can also be seen that having only one mixer

always results in a much higher completion time while having more than enough mixers (four mixers for three reactions) results in the lowest completion time.

## 5.4 Continuous Mode Reactions

For a dual ring layout with  $e_o = 60$  and  $e_i = 24$ , multiple droplets of each reactant were allowed to enter the system as and when space was available in the outer ring. With one mixer, 3 droplets of each reactant could be introduced before deadlock was reached. With two mixers, this number increased to 4 and with three mixers, it further increased to 5. Thus, as expected, increasing the number of mixers can allow more reactions to happen in parallel without congesting the system. This is important in the case of continuous mode reactions where the reactants are introduced into the system at a constant input rate.

## 5.5 Comparison of Dual and Synchronous Ring Layouts

We carried out some example analyses on both kinds of ring layouts for a preliminary comparison. For three independent reactions on a synchronous ring layout, the mixing and the reaction times were kept as before and each ring used four phases. The reservoirs were arranged such that the two sources and the sink for a reaction were all attached to the same unit as shown in Fig. 5.2. This was done to reduce transportation time. There are a total of 4 units and 10 reservoirs in this example. The completion time was found to be 87 clock cycles. Even though there are 4 mixers available, only 3 of them get used as there are only 3 reactions to be carried out. Comparing this completion time to the results of the dual ring layout, we find that the dual ring layout takes much more time for completion with a single mixer (194 clock cycles). Even with 4 mixers, the dual ring layout takes 137 clock cycles. Of course, rearrangement of the reservoirs in the dual ring layout may help in reducing the completion time. For example, if all sinks are placed close to the interconnections in the anticlockwise direction, then transportation time of final product droplets can be reduced.

One more thing to note is that the synchronous ring layout uses only 43 phases while the dual ring layout uses 59 phases with 4 mixers (52 phases with 3 mixers).

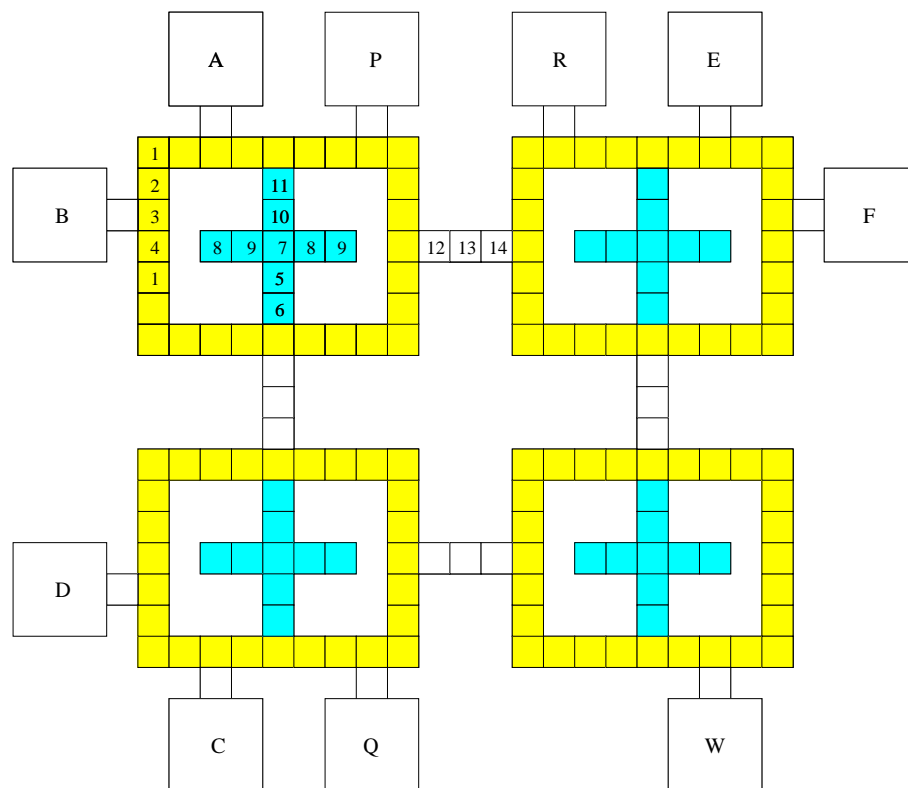


**Figure 5.2: Synchronous ring layout with bus-phase addressing used for our simulations. The reservoirs for any two reactants forming a compatible pair and the corresponding product are all attached to the same unit to reduce transportation time. Thus, the reservoirs for *A*, *B*, and *P* are all attached to the same outer ring.**

Thus, there is a significant reduction in the number of phases required for the synchronous ring layout.

In the synchronous ring layout, since there is no inner ring, completion of the chemical reaction happens in the outer ring itself. Thus, the chemical reaction process gets combined with transportation and the final product droplet may end up much closer to its sink at the end of its chemical reaction. This helps in reducing the transportation time on the chip.

Also, if multiple droplets of reactants are allowed to be injected on a synchronous ring layout as and when space become available, chances of deadlock become much lower as compared to dual ring layout. This is because the reactant droplets are now distributed among many rings (of different units). So, a single ring is being shared by a much smaller number of droplets making congestion less likely.

## 6. HARDWARE IMPLEMENTATION

### 6.1 Hardware Interface Design

One of the main goals of our research is to interface our algorithm with actual DMFS chips so that the control of the DMFS system for biochemical analysis becomes completely automated. We have been working on designing and building hardware to interface our algorithm with DMFS chips as shown in Fig. 6.1.



**Figure 6.1:** A logical representation of the relationship between the algorithm, hardware interface, and the DMFS chip.

The basic idea is to generate a binary signal for each phase at each clock cycle using the algorithm and then use these signals to supply either a 100V RMS or a 0V signal to the corresponding electrodes. The interface would consist of high-voltage switches controlled by the binary signals as shown in Fig. 6.2. If the binary signal is a 1, the switch turns ON thereby causing 100V RMS to be applied to the contact pad connected to it, and if the binary signal is a 0, it turns OFF thereby causing 0V to be applied to the connected contact pad. The number of these switches needs to be equal to the number of phases on the chip.

### 6.2 DMFS Control Electronics Setup

We have assembled and successfully tested the complete electronics setup<sup>3</sup> (shown in Fig. 6.3) required for *manual* activation of electrodes on a DMFS. The individual components of this setup are listed below:

1. Agilent 33220A Function Generator: Used to generate a sine wave signal of

---

<sup>3</sup>This work has been done with assistance from Prof. Aaron Wheeler's group at the University of Toronto.

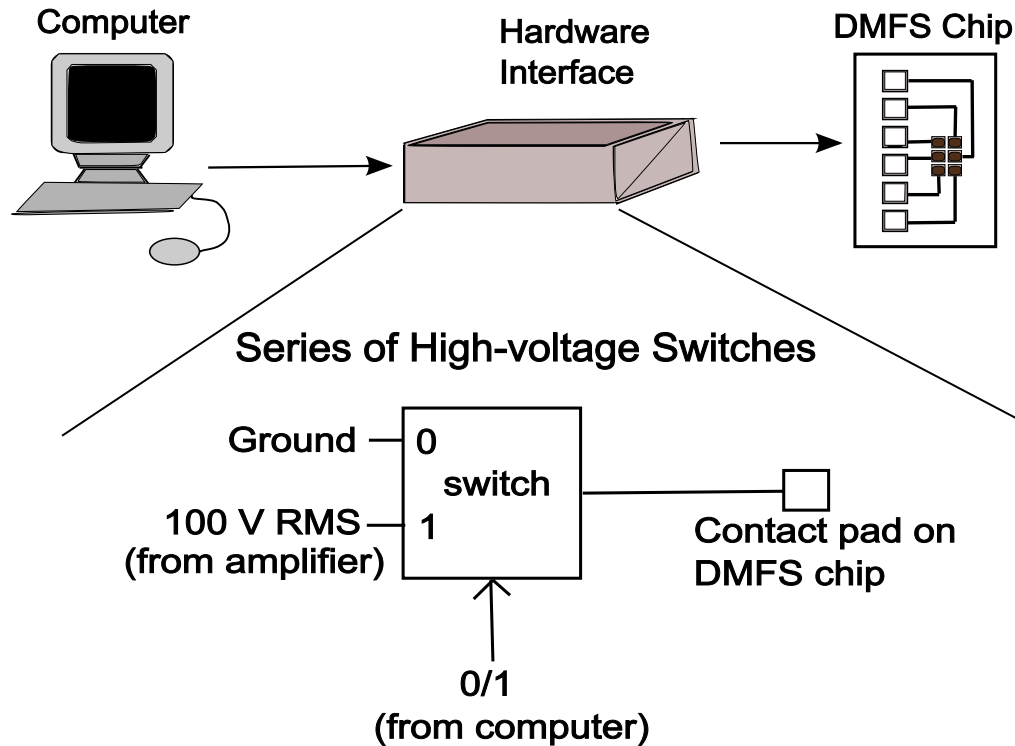


**Figure 6.2: Hardware interface**

less than 10V peak-to-peak amplitude and 18 kHz frequency. This signal is then fed into a high voltage amplifier that has a gain of 200V/V.

2. Trek, Inc. Model PZD700-2-L-CE Two-Channel High Voltage Amplifier: Generates a high-voltage signal that is applied to the contact pads on a DMFS chip to activate the corresponding electrodes. The output of the function generator is adjusted so that the amplifier output is about 100V RMS.
3. Agilent DSO3062A, 2 Channel 60 MHz 1GSa/s Oscilloscope: Helps observe the input and output waveforms.
4. EO-1312C Color USB Camera (Model No. NT59-366), KC InFocus Micro Video Lens (Model No. NT53-785), KC Objective IF-3 Lens (Model No. NT53-783), Standard Boom Stand (Model No. NT54-120), 1/4-20 Mounting Plate (Model No. NT54-122), and EO USB Cam 1/4-20 Mounting Plate (Model No. NT59-473) from Edmund Optics: Eases observation of droplet movement on DMFS chips and helps record videos.



**Figure 6.3:** Electronic setup for manual activation of electrodes.

### 6.3 DMFS Chip Fabrication

We have developed the capability to fabricate DMFS chips at RPI<sup>4</sup>. The step-by-step fabrication process of the DMFS chip described in [24] is given below. A first prototype fabricated using this procedure is shown in Fig. 6.4. It consists of 14 electrodes in all (squares on the left in the figure), 2 of which are used as reservoirs (the big squares). The 14 squares on the right in the figure are the contact pads, one for each electrode, used to activate the corresponding electrodes. The complete fabrication process is also depicted in Fig. 6.5.

1. Clean the glass slides in piranha solution (7:3 concentrated sulfuric acid/30% hydrogen peroxide) for 10 min.
2. Coat slides with chromium (10 nm) by electron beam deposition.
3. Coat slides with gold (100 nm) by electron beam deposition.
4. Rinse slides with acetone, methanol, and DI water.

---

<sup>4</sup>This work has been done by Jeff Martin at RPI with assistance from Prof. Aaron Wheeler's group at the University of Toronto.



5. Bake slides on a hot plate (115 C, 5 min).
6. Spin-coat the substrates with HMDS (3000 rpm, 30 s).
7. Spin-coat with Shipley S1811 photoresist (3000 rpm, 30 s).
8. Bake substrates on a hot plate (100 C, 2 min).
9. Expose substrates through a photomask using a Suss Mikrotek mask aligner (35.5 mW/cm<sup>2</sup>, 365 nm, 3 s).
10. Immerse substrates in MF321 developer for 3 min.
11. Postbake substrates on a hot plate (100 C, 1 min).
12. Immerse substrates in gold etchant (50 s) followed by chromium etchant (30 s).
13. Strip the remaining photoresist in AZ300T for at least 5 min in an ultrasonic cleaner.
14. Coat with 1  $\mu$  m of parylene-C.
15. Coat with 50 nm of Teflon-AF.

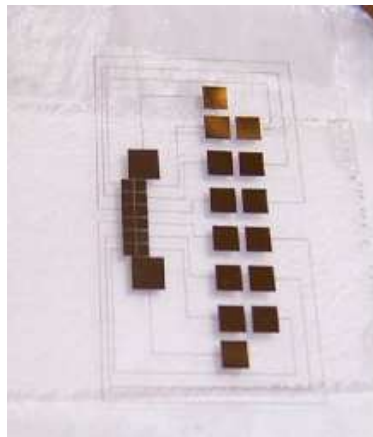


**Figure 6.4:** A directly addressable DMFS chip fabricated at RPI.

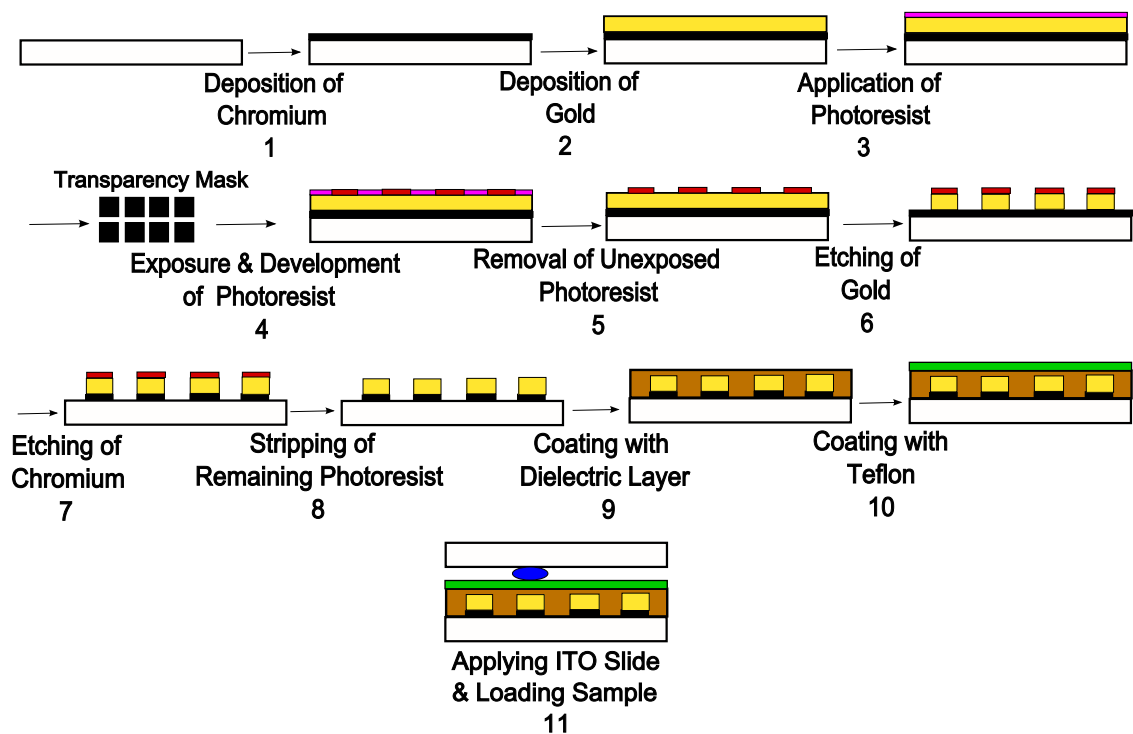


Figure 6.5: Chip fabrication process.

## 6.4 Design of Layout for Synthesis of Heparin

Using the technologies of digital microfluidics, the microscale enzymatic synthesis of the heparin glycan will be carried out from the starting substrate heparosan, as expressed by *E. coli* K5. Heparosan is immobilized on streptavidin nanoparticles. The heparosan substrate will be then enzymatically modified with C5-epimerase, 2-O-sulfotransferase (2-OST), 6-OST, and 3-OST to yield the final product, heparin. The heparin will then be bound to a fluorescent protein like Antithrombin-III (AT-III) for visualization and detection. The microfluidic system will be used for the controlled synthesis of the heparin glycan, much like the natural complex process of glycan synthesis occurring in the Golgi organelle. The synthesis of heparin can be viewed as a linear chain reaction as shown in Fig. 6.6. The detailed step-by-step reaction can be found in Fig. 5 of [14].

We have come up with a customized design for a directly-addressable (each electrode controlled by an independent signal) DMFS chip for the synthesis of heparin. The design utilizes the fact that heparin synthesis is a chain reaction where

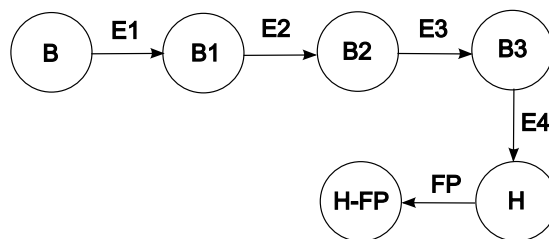


Figure 6.6: Simplified diagram of heparin synthesis. *E1*, *E2*, *E3*, and *E4* represent the enzymes that modify the original Streptavidin beads *B* into *B1*, *B2*, *B3*, and finally *H* where *H* stands for the final product *heparin*. Heparin is then bound to a fluorescent protein *FP* for easy visualization. *H-FP* represents heparin bounded to the fluorescent protein.

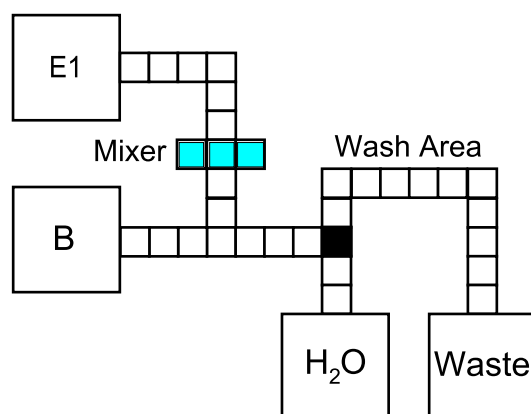
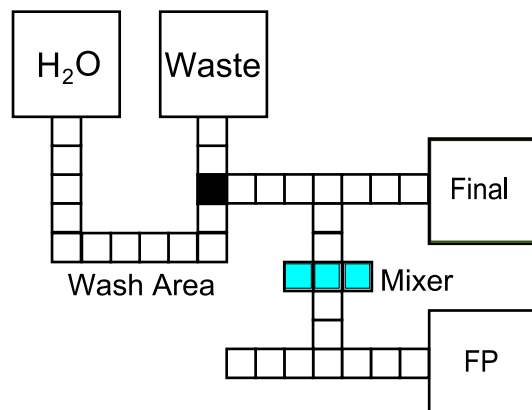


Figure 6.7: The starting unit of the layout for heparin synthesis. *E1* stands for the first enzyme and *B* represents magnetic beads in solution. 600 nm Streptavidin beads will be used for heparin synthesis.

600nm Streptavidin magnetic beads are treated with a different enzyme at every stage of the chain and then washed with water to eliminate any traces of the enzyme from the preceding stage sticking to the beads. The layout consists of repeating units where each unit is used to carry out one stage of the reaction.

The first unit of the layout is shown in Fig. 6.7 where the magnetic beads *B* will be treated with the first enzyme *E1* in the mixer and then washed with water in the wash area. The black electrode in the figure represents an electrode with a magnet attached to it. When a droplet containing both the modified beads and unused enzyme reaches this electrode, the magnet will hold the beads in place while a droplet containing only unused enzyme will move ahead as the adjacent electrodes are activated. Thus, the modified beads get separated from the unused enzyme.



**Figure 6.8:** The last unit of the layout for heparin synthesis. *FP* stands for fluorescent protein and *Final* represents the final product obtained.

After being washed with water, the beads are ready to be treated with the next enzyme.

The last unit of the layout is shown in Fig. 6.8 where the final product of the chain reaction will be first bound to a fluorescent protein *FP* for visualization and then sent to the sink labeled *Final*. Keeping the first and the last unit always the same, such units can be replicated and combined to obtain a layout as shown in Fig. 6.9 to carry out the chain reaction upto any desired stage. *E1*, *E2*, and *E3* in Fig. 6.9 stand for the enzymes with which the beads *B* are treated successively.

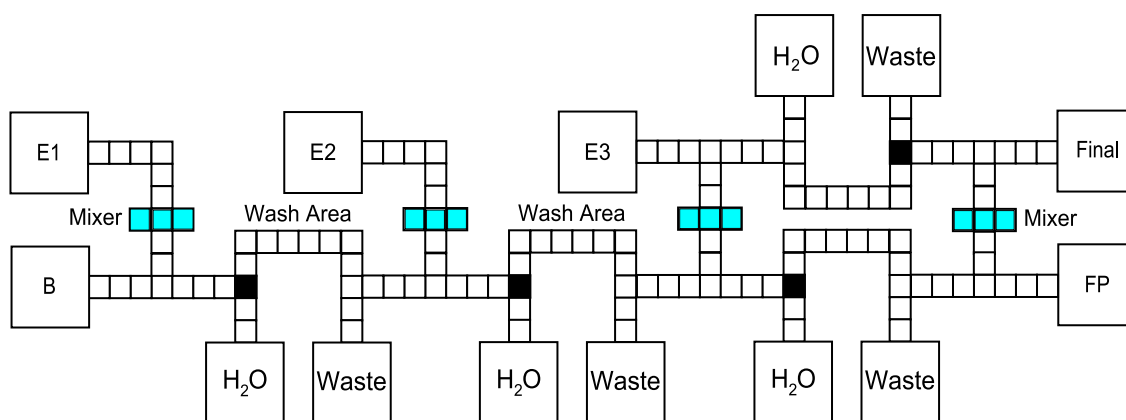


**Figure 6.9:** The layout formed by concatenating units together. A chain reaction can be carried out on this layout with each stage of the reaction occurring on a different unit.

## 7. CONCLUSIONS AND FUTURE WORK

We have presented an approach to carry out batch mode operations on ring layouts with bus-phase addressing. We have successfully demonstrated automated independent and chain reactions in simulation and identified possible deadlock scenarios. The algorithm allows a variety of chemical analyses to occur in parallel on a given ring layout and also works for layouts with multiple mixers and inner rings, different numbers of reservoirs, and different phase assignments.

The current algorithm can be optimized by relaxing many of the simplifying assumptions. For example, droplet movement from the outer ring to the inner ring can be permitted to reduce transportation time to the mixer. Waste droplets can be allowed to leave the mixer via the inner ring. Both clockwise and anticlockwise movement can be permitted in both the rings. For a reaction with no sensor constraints, the droplet undergoing a reaction can be transported to its destination while the reaction goes to completion. Mixing times and reaction times can be taken into account while choosing the droplet pair to be sent to the mixer to get a more efficient scheduling strategy.

Changes to the ring layout such as multiple instances of the ring layout connected together can permit a greater number of reactions to take place on the array. Automating continuous mode reactions is another important goal. Optimum input rate and placement of components need to be identified to avoid congestion and deadlocks. Finding an optimum schedule to minimize completion time and generalizing the algorithm to control arbitrary layouts with bus-phase addressing pose very interesting challenges.

## REFERENCES

- [1] K. F. Böhringer. Towards optimal strategies for moving droplets in digital microfluidic systems. In *IEEE International Conference on Robotics and Automation*, New Orleans, LA, Apr. 2004.
- [2] K. F. Böhringer. Modeling and controlling parallel tasks in droplet-based microfluidic systems. *IEEE Transactions on Computer-Aided Design of Integrated Circuits and Systems*, 25:334–344, Feb. 2006.
- [3] S. K. Cho, H. Moon, and C.-J. Kim. Creating, transporting, cutting, and merging liquid droplets by electrowetting-based actuation for digital microfluidic circuits. *Journal of Microelectromechanical Systems*, 12(1):70–80, Feb. 2003.
- [4] J. Ding, K. Chakrabarty, and R. B. Fair. Scheduling of microfluidic operations for reconfigurable two-dimensional electrowetting arrays. *IEEE Transactions on Computer-Aided Design of Integrated Circuits and Systems*, 20(12):1463–1468, Dec. 2001.
- [5] P. S. Dittrich and A. Manz. Lab-on-a-chip: microfluidics in drug discovery. *Nature Reviews Drug Discovery*, 5(3):210–218, Mar. 2006.
- [6] R. B. Fair, V. Srinivasan, H. Ren, P. Paik, V. Pamula, and M. G. Pollack. Electrowetting-based on-chip sample processing for integrated microfluidics. In *IEEE International Electron Devices Meeting (IEDM)*, pages 779–782, 2003.
- [7] S.-K. Fan, C. Hashi, and C.-J. Kim. Manipulation of multiple droplets on NxM grid by cross-reference EWOD driving scheme and pressure-contact packaging. In *IEEE Conference on MEMS*, pages 694–697, Kyoto, Japan, Jan. 2003.
- [8] P. R. C. Gascoyne, J. V. Vykoukal, J. A. Schwartz, T. J. Anderson, D. M. Vykoukal, K. W. Current, C. McConaghy, F. K. Becker, and C. Andrews. Dielectrophoresis-based programmable fluidic processors. *Lab on a Chip*, 4(4):299–309, Aug. 2004.
- [9] J. Gong, S.-K. Fan, and C.-J. Kim. Portable digital microfluidics platform with active but disposable lab-on-chip. In *Tech. Digest of 17th IEEE International Conference on Micro Electro Mechanical Systems*, pages 355–358, Maastricht, The Netherlands, Jan. 2004.

- [10] J. Gong and C.-J. Kim. Two-dimensional digital microfluidic system by multi-layer printed circuit board. In *Proceedings of IEEE MEMS 2005*, pages 726–729, Miami, Florida, Jan. 2005.
- [11] E. J. Griffith and S. Akella. Coordinating multiple droplets in planar array digital microfluidic systems. *International Journal of Robotics Research*, 24(11):933–949, Nov. 2005.
- [12] E. J. Griffith, S. Akella, and M. K. Goldberg. Performance characterization of a reconfigurable planar-array digital microfluidic system. *IEEE Transactions on Computer-Aided Design of Integrated Circuits and Systems*, 25(2):340–352, Feb. 2006.
- [13] T. B. Jones, M. Gunji, M. Washizu, and M. J. Feldman. Dielectrophoretic liquid actuation and nanodroplet formation. *Journal of Applied Physics*, 89:1441–1448, Jan. 2001.
- [14] R. J. Linhardt, J. S. Dordick, P. L. DeAngelis, and J. Liu. Enzymatic synthesis of glycosaminoglycan heparin. In *Seminars in Thrombosis and Hemostasis*, volume 33, pages 453–465, 2007.
- [15] N. Manaresi, A. Romani, G. Medoro, L. Altomare, A. Leonardi, M. Tartagni, and R. Guerrieri. A CMOS chip for individual cell manipulation and detection. *IEEE Journal of Solid-State Circuits*, 38(12):2297–2305, Dec. 2003.
- [16] P. Paik, V. K. Pamula, and R. B. Fair. Rapid droplet mixers for digital microfluidic systems. *Lab on a Chip*, 3:253–259, 2003.
- [17] R. Pal, M. Yang, R. Lin, B. N. Johnson, N. Srivastava, S. Z. Razzacki, K. J. Chomistek, D. C. Heldsinger, R. M. Haque, V. M. Ugaz, P. K. Thwar, Z. Chen, K. Alfano, M. B. Yim, M. Krishnan, A. O. Fuller, R. G. Larson, D. T. Burke, and M. A. Burns. An integrated microfluidic device for influenza and other genetic analyses. *Lab Chip*, 5(10):1024–1032, Oct. 2005.
- [18] M. G. Pollack, R. B. Fair, and A. D. Shenderov. Electrowetting-based actuation of liquid droplets for microfluidic applications. *Applied Physics Letters*, 77:1725–1726, 2000.
- [19] M. G. Pollack, P. Y. Paik, A. D. Shenderov, V. K. Pamula, F. S. Dietrich, and R. B. Fair. Investigation of electrowetting-based microfluidics for real-time PCR applications. In *Seventh International Conference on Miniaturized Chemical and Biochemical Analysis Systems (MicroTAS '03)*, Squaw Valley, CA, Oct. 2003.
- [20] V. Srinivasan, V. Pamula, M. Pollack, and R. Fair. A digital microfluidic biosensor for multianalyte detection. In *IEEE 16th Annual International Conference on Micro Electro Mechanical Systems*, pages 327–330, 2003.

- [21] V. Srinivasan, V. K. Pamula, and R. B. Fair. An integrated digital microfluidic lab-on-a-chip for clinical diagnostics on human physiological fluids. *Lab on a Chip*, 4:310–315, 2004.
- [22] F. Su and K. Chakrabarty. Architectural-level synthesis of digital microfluidics-based biochips. In *Proc. IEEE International Conference on CAD*, pages 223–228, 2004.
- [23] O. D. Velev, B. G. Prevo, and K. Bhatt. On-chip manipulation of free droplets. *Nature*, 426:515–516, 2003.
- [24] M. W. L. Watson, M. Abdelgawad, G. Ye, N. Yonson, J. Trottier, and A. R. Wheeler. Microcontact printing-based fabrication of digital microfluidic devices. *Analytical Chemistry*, 78:7877–7885, 2006.
- [25] A. R. Wheeler, H. Moon, C.-J. C. Kim, J. A. Loo, and R. L. Garrell. Electrowetting-based microfluidics for analysis of peptides and proteins by matrix-assisted laser desorption/ionization mass spectrometry. *Analytical Chemistry*, 76(16):4833–4838, Aug. 2004.
- [26] T. Xu and K. Chakrabarty. Droplet-trace-based array partitioning and a pin assignment algorithm for the automated design of digital microfluidic biochips. In *Proc. IEEE/ACM International Conference on Hardware/Software Codesign and System Synthesis*, pages 112–117, 2006.